Using reciprocity to derive the far field displacements due to buried sources and scatterers

L. R. Francis Rose[a)]
Aerospace Division, Defence Science and Technology Group, 506 Lorimer Street, Fishermen's Bend, Melbourne, Victoria 3207, Australia

W. K. Chiu, N. Nadarajah, and B. S. Vien
Department of Mechanical and Aerospace Engineering, Monash University, Wellington Road, Clayton, Victoria 3800, Australia

(Received 4 July 2017; revised 24 September 2017; accepted 18 October 2017; published online 15 November 2017)

It is shown that elastodynamic reciprocity provides a simpler approach for deriving the far-field displacements due to buried (sub-surface) sources in a half-space, compared with integral transform techniques. The auxiliary fields employed in this approach are the fields associated with the reflection of plane waves of the three possible polarisations, and the required far field can be expressed in terms of these well-known auxiliary fields. The crucial step in this approach is to evaluate a surface integral involving cross-work terms between an outgoing spherical wavefront and the auxiliary fields consisting of incident and reflected plane waves. This integral can be evaluated by the stationary phase approximation for the two-dimensional case, or by a generalisation of this approximation for the three-dimensional case. Although this evaluation involves several distinct contributions, the final result is shown to be very simple, and it can be interpreted as a generalisation of a known result for the one-dimensional case, whereby the net contribution arises only from counter-propagating waves of the same mode. The results derived for a buried force are extended to the case of buried cracks by exploiting the body force equivalents for displacement discontinuities across a surface. https://doi.org/10.1121/1.5009666

[ANN] Pages: 2979–2987

I. INTRODUCTION

Achenbach[1] has recently presented an extensive discussion of elastodynamic reciprocity, including several examples of practical applications.[2–10] He noted that the solutions obtained via reciprocity can often be derived in an equally simple or simpler manner by other approaches, notably integral transform techniques. However, that is not the case for buried source problems in a half-space, or half-plane, for which reciprocity provides a simpler and more elegant approach. This has been illustrated for laser-generated ultrasound,[5,6] and more recently for a Mode I crack as a source of acoustic emission.[10] However, these illustrations have focussed on deriving only the surface wave motions due to those sources. In many contexts, it is also of interest to characterise the far-field bulk-wave radiation or scattering patterns due to buried sources or scatterers. The aim of this paper is to show that an application of reciprocity again provides a simple and elegant approach for this purpose.

The appropriate auxiliary solution that will be employed is the well-known solution for the reflection of a plane wave at the traction-free boundary of a half-space (or half-plane).[11–13] For the two-dimensional (2D) case, the crucial step in implementing the reciprocity approach turns out to be the use of the stationary phase approximation to evaluate the cross-work term between an outgoing circular wavefront, and the (total) field due to an incoming plane wave. For the three-dimensional (3D) case, a multi-dimensional extension of the stationary phase approximation is required to evaluate this cross-work term between an outgoing spherical wavefront and the field due to an incoming plane wave. In both cases, a detailed consideration of all the contributions to this cross-work term is lengthy, but the final result conforms to a simple rule that is a straightforward generalisation of a known result for the one-dimensional case.[1]

The present work is motivated by applications to structural health monitoring[14,15] where it is of interest to characterise Lamb wave scattering by cracks and delaminations in plate-like structures, particularly when these forms of damage occur at or near the boundary of a hole or a straight edge.[16–19] Representations for the scattered field due to cracks and delaminations have the same form as the representations for the radiated field due to crack-like sources, except that the source density is an induced source density that depends on the incident field.[20–25] In general, this induced source density can only be determined computationally,[26–30] but it is often sufficient to estimate the source density by using, for example, a quasi-static approximation that is appropriate in the short crack (or long wavelength) limit.[31] Indeed, in that limit, the radiated or scattered field from a crack can be approximated by a point source consisting of a particular combination of force doublets (or dipoles), which represents the field due to an infinitesimal crack element.[20–23] The present work will only consider in detail the field for a buried force or crack element in a half-plane or

[a)]Electronic mail: francis.rose@dst.defence.gov.au

half-space, but it will be clear that the approach is also advantageous for any configuration for which there is a convenient analytical solution for the field due to an incident plane wave. This includes therefore the case of cracks and delaminations at or near the boundary of circular or spherical holes.[32]

The paper is organised as follows. The buried source problem is formulated in Sec. II for a 2D point force (or line load), and a solution based on reciprocity is presented. The key step in deriving this solution is considered in detail in Sec. III, where it is shown that an application of the stationary phase approximation leads to a simple rule for evaluating the cross-work surface integral. This approach is extended to the 3D problem for a buried force in Sec. IV, which requires an extension of the stationary phase approximation to multi-dimensional integrals.[33,34] This solution serves as the building block for the representation of the radiated or scattered field due to various sources or scatterers. The case of a 3D crack-like scatterer is considered in Sec. V where it is shown that reciprocity leads to a compact representation for the far-field displacements. These compact representations for buried sources constitute the novelty in the present work relative to the existing literature. Finally, some straightforward generalisations of the present approach are briefly noted in Sec. VI.

II. SOLUTION FOR A TWO-DIMENSIONAL BURIED FORCE

The reciprocal theorem for time-harmonic elastic fields can be stated as follows (Ref. 1, Sec. 6.2):

$$\int_V (\boldsymbol{f}^A \cdot \boldsymbol{u}^B - \boldsymbol{f}^B \cdot \boldsymbol{u}^A) dV = \int_S (\boldsymbol{T}^B \cdot \boldsymbol{u}^A - \boldsymbol{T}^A \cdot \boldsymbol{u}^B) dS, \tag{1}$$

where $\boldsymbol{u}, \boldsymbol{f}$ denote, respectively, the elastic displacement and the body force for two states identified by the superscripts A, B, with the time factor $e^{-i\omega t}$ omitted, and $\boldsymbol{T}$ denotes the corresponding traction vector, i.e., $T_i = \sigma_{ji} n_j$ where σ_{ij} denotes the stress tensor, $\boldsymbol{n} = n_j$ the outward normal to the closed surface S, and the summation convention over repeated subscripts applies. To illustrate the application of this theorem for buried sources, consider first the 2D plane strain problem for a point force in an isotropic half-plane. State A is chosen to be the solution of the equations of motion

$$(\lambda + \mu) \nabla\nabla \cdot \boldsymbol{u} + \mu \nabla^2 \boldsymbol{u} + \rho\omega^2 \boldsymbol{u} = -\boldsymbol{f}, \tag{2a}$$

where λ, μ denote the Lamé parameters, ρ the density, and the body force is given by

$$\begin{aligned} f_x &= P\delta(x)\delta(y - l), \\ f_y &= 0, \end{aligned} \tag{2b}$$

with δ denoting the Dirac delta function, corresponding to a horizontal force as shown in Fig. 1. This solution is subject to the traction-free boundary condition

$$\boldsymbol{T} = \boldsymbol{0} \quad \text{on} \quad y = 0, \tag{2c}$$

and the requirement of representing outgoing waves, in accordance with the Sommerfeld radiation condition. The far field can therefore be expected to consist of outgoing

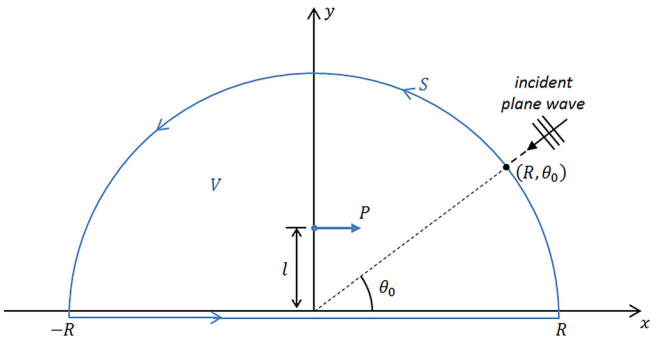

FIG. 1. (Color online) The two-dimensional configuration for a buried point force in a half-plane $y \geq 0$ showing the volume V and surface S employed in Eq. (1), as well as the incident plane wave that generates the required auxiliary field.

longitudinal and transverse waves travelling with speeds c_L, c_T, respectively, and with amplitude exhibiting the characteristic inverse-square-root spatial decay for 2D wave motion. Thus, an appropriate ansatz for the far field is

$$\begin{aligned} u_r^A &\approx A_x^L(\theta)\Omega(k_L r), \\ u_\theta^A &\approx A_x^T(\theta)\Omega(k_T r), \\ \Omega(kr) &= \sqrt{\frac{i}{8\pi kr}} e^{ikr}, \end{aligned} \tag{3}$$

where r, θ denote polar coordinates, $k_L = \omega/c_L, k_T = \omega/c_T$ the wavenumbers, and the symbol $\approx$ is used here and in the sequel to denote asymptotic equality, i.e., omitting terms that are asymptotically negligible compared with the retained term for $kr \gg 1$, where $k = k_L$ or k_T. The functions A^L, A^T characterising the angular dependence remain to be determined.

Before proceeding, it is noted that the function Ω in Eq. (3) is the far-field asymptotic expansion of the free-space Green function for the 2D scalar wave equation. More precisely, this Green function is the solution of

$$\nabla^2 G + k^2 G = -\delta(x)\delta(y), \tag{4a}$$

that satisfies the Sommerfeld radiation condition. This solution is given by (Ref. 1, Sec. 6.6)

$$G(r, \theta) = \frac{i}{4} H_0^{(1)}(kr) \approx \Omega(kr). \tag{4b}$$

This choice for the radial dependence in the ansatz corresponds to that used for defining the scattering amplitude in the context of diffraction tomography.[35–38]

State B is chosen to be the field due to an incident plane wave that also satisfies the traction-free boundary condition in Eq. (2c). More precisely, to determine A_x^L, the incident wave must be chosen to be a longitudinal wave (P-wave) of unit amplitude, given by

$$\begin{aligned} \boldsymbol{u}^{IL}(x, y) &= \boldsymbol{d}_0 e^{ik_L \boldsymbol{\alpha} \cdot \boldsymbol{x}}, \\ \boldsymbol{d}_0 &= \boldsymbol{\alpha} = -(\cos\theta_0, \sin\theta_0), \end{aligned} \tag{5}$$

with $\boldsymbol{\alpha}$ denoting the unit vector in the direction of propagation, as indicated schematically in Fig. 1, and $\boldsymbol{d}_0$ the unit vector characterising the polarisation of the incident wave. The total field due to this incident wave will be denoted by

$\boldsymbol{u}^{BL}(x,y;\theta_0)$. This field is well known.[1,11–13] It consists of the incident wave and two reflected plane waves, as follows:

$$\boldsymbol{u}^{BL}(x,y;\theta_0) = \boldsymbol{u}^{IL} + A_{11}\boldsymbol{u}^{RL} + A_{21}\boldsymbol{u}^{RT}, \tag{6a}$$

$$\boldsymbol{u}^{RL} = \boldsymbol{d}_1 e^{ik_L\boldsymbol{\beta}\cdot\boldsymbol{x}}, \quad \boldsymbol{\beta} = \boldsymbol{d}_1 = -(\cos\theta_0, \sin\theta_0), \tag{6b}$$

$$\boldsymbol{u}^{RT} = \boldsymbol{d}_2 e^{ik_T\boldsymbol{\gamma}\cdot\boldsymbol{x}}, \quad \boldsymbol{\gamma} = (-\sin\psi_0, \cos\psi_0),$$
$$\boldsymbol{d}_2 = -(\cos\psi_0, \sin\psi_0), \tag{6c}$$

$$\kappa\sin\psi_0 = \cos\theta_0, \quad \kappa = c_L/c_T = [2(1-\upsilon)/(1-2\upsilon)]^{1/2}, \tag{6d}$$

$$A_{11} = (\sin 2\phi_0 \sin 2\psi_0 - \kappa^2\cos^2 2\psi_0)/D, \tag{6e}$$

$$A_{21} = (2\kappa \sin 2\phi_0 \cos 2\psi_0)/D, \tag{6f}$$

$$\phi_0 = \pi/2 - \theta_0, \quad D = \sin 2\phi_0 \sin 2\psi_0 + \kappa^2\cos^2 2\psi_0. \tag{6g}$$

The key features of this solution are (i) the x-component of the reflected wave vectors must be equal to that of the incident wave, in accordance with Snell's law; (ii) the propagation vectors $\boldsymbol{\beta}, \boldsymbol{\gamma}$, and polarisations are therefore given by Eqs. (6b), (6c), and the reflection coefficients A_{11}, A_{21}, are readily derived from the boundary condition Eq. (2c). Because the geometry does not involve any characteristic lengths, these reflection coefficients do not depend on frequency (or wavelength): they only depend on the angle of incidence θ_0 (measured from the x axis, as indicated in Fig. 1), and the Poisson ratio υ, through the parameter κ defined in Eq. (6d).

On applying Eq. (1) to these two states, one finds that the left-hand side (LHS) reduces to $Pu_x^{BL}(0,l;\theta_0)$, by virtue of Eq. (2b) and noting that $\boldsymbol{f}^B = \boldsymbol{0}$, whereas the right-hand side (RHS) will be shown in Sec. III to reduce to $-(\lambda+2\mu)A_x^L(\theta_0)$, thereby leading to

$$A_x^L(\theta_0) = -\frac{1}{\lambda+2\mu} Pu_x^{BL}(0,l;\theta_0). \tag{7}$$

Next, to determine A_x^T in Eq. (3), the incident wave is chosen to be a transverse wave of unit amplitude incident at an angle θ_0 to the x axis, as specified by

$$\boldsymbol{u}^{IT}(x,y) = \boldsymbol{d}_0 e^{ik_T\boldsymbol{\alpha}\cdot\boldsymbol{x}},$$
$$\boldsymbol{\alpha} = -(\cos\theta_0, \sin\theta_0), \quad \boldsymbol{d}_0 = (\sin\theta_0, -\cos\theta_0). \tag{8}$$

The total field can again be expressed as the sum of three plane waves, as follows:[1,11–13]

$$\boldsymbol{u}^{BT}(x,y;\theta_0) = \boldsymbol{u}^{IT} + A_{12}\boldsymbol{u}^{RL} + A_{22}\boldsymbol{u}^{RT}, \tag{9a}$$

$$\boldsymbol{u}^{RL} = \boldsymbol{d}_1 e^{ik_L\boldsymbol{\beta}\cdot\boldsymbol{x}}, \quad \boldsymbol{\beta} = \boldsymbol{d}_1 = (-\sin\phi_0, \cos\phi_0),$$
$$\sin\phi_0 = \kappa\cos\theta_0, \tag{9b}$$

$$\boldsymbol{u}^{RT} = \boldsymbol{d}_2 e^{ik_T\boldsymbol{\gamma}\cdot\boldsymbol{x}}, \quad \boldsymbol{\gamma} = (-\cos\theta_0, \sin\theta_0),$$
$$\boldsymbol{d}_2 = -(\sin\theta_0, \cos\theta_0), \tag{9c}$$

$$A_{12} = -(\kappa\sin 4\psi_0)/D, \tag{9d}$$

$$A_{22} = (\sin 2\phi_0 \sin 2\psi_0 - \kappa^2\cos^2 2\psi_0)/D, \tag{9e}$$

$$\psi_0 = \pi/2 - \theta_0, \quad D = \sin 2\phi_0 \sin 2\psi_0 + \kappa^2\cos 2\psi_0. \tag{9f}$$

It is noted that in this case, the character of the solution is different for values of the incident angle θ_0 below a critical value θ_c defined by $\kappa\sin\theta_c = 1$. For $\theta_0 = \theta_c$ the reflected longitudinal wave is at grazing incidence, i.e., the wave vector is aligned with the negative x axis; for $0 < \theta_0 < \theta_c$, the reflected longitudinal wave is an inhomogeneous plane wave, still propagating in the direction of the negative x axis, but with an amplitude that decays exponentially with depth y from the boundary $y = 0$.

With this choice for the B-state, and the ansatz in Eq. (3) for the A-state, Eq. (1) now leads to

$$A_x^T(\theta_0) = -\frac{1}{\mu} Pu_x^{BT}(0,l;\theta_0). \tag{10}$$

Thus, it can be seen that an application of reciprocity leads to a compact expression for the angular dependence of the far field due to a buried horizontal force, involving only the well-known solution for plane wave reflection in a half-plane. Furthermore, the notation clearly suggests how the result might be extended to a point force of arbitrary direction. The preceding analysis can be repeated for a vertical force, leading to the same results as in Eqs. (7) and (10), but with the x-component of the B-field replaced by the y-component.

These results can now be combined to obtain the far-field solution of Eqs. (2a) for an arbitrarily directed body force acting at an arbitrary point $\boldsymbol{\xi}$, as specified by

$$\boldsymbol{f} = \boldsymbol{F}\delta(\boldsymbol{x} - \boldsymbol{\xi}) \tag{11a}$$

in a half-plane $y \geq 0$ subject to the traction-free boundary condition Eq. (2c) and the Sommerfeld radiation condition, in the following form:

$$u_r(r,\theta) \approx A^L(\theta)\Omega(k_L r), \tag{11b}$$

$$u_\theta(r,\theta) \approx A^T(\theta)\Omega(k_T r), \tag{11c}$$

$$A^L(\theta_0) = -\frac{1}{\lambda+2\mu}\boldsymbol{F}\cdot\boldsymbol{u}^{BL}(\boldsymbol{\xi};\theta_0), \tag{11d}$$

$$A^T(\theta_0) = -\frac{1}{\mu}\boldsymbol{F}\cdot\boldsymbol{u}^{BT}(\xi;\theta_0), \tag{11e}$$

where $\boldsymbol{u}^{BL}$ and $\boldsymbol{u}^{BT}$ are the fields given by Eqs. (6) and (9), corresponding to the reflection of an incident longitudinal or transverse plane wave, respectively.

It is worth pointing out that the preceding derivation based on reciprocity is definitely simpler than the alternative approach based on integral transforms, which would require a separate representation for the potentials in the domains $0 \leq y < l$ and $l < y < \infty$, leading to a requirement to solve a set of six simultaneous equations for six unknown coefficients, so as to satisfy the matching and boundary conditions on $y = l$ and $y = 0$.[39,40] By contrast, for the case of surface forces, the integral transform approach would only require

the solution of two simultaneous equations for two unknown coefficients, which can be considered to be a comparable level of simplicity to the solution for plane wave reflection that also requires the solution of two simultaneous equations to determine the reflection coefficients.

III. EVALUATION OF THE SURFACE INTEGRAL

We return now to evaluating the surface integral on the RHS of Eq. (1) for the case of a horizontal force and an incident longitudinal wave, i.e., for state A given by Eq. (3) and state B by Eq. (6). The surface S is taken to be a closed curve consisting of a straight segment $-R < x < R$ along the x axis, closed by a semi-circle of radius R, as shown in Fig. 1. The integral along the straight segment vanishes in view of the traction-free boundary condition Eq. (2c) that applies for both states, leaving only the integral around the semi-circle.

Consider first the contribution from the second term on the RHS of Eq. (1), which leads to

$$\begin{aligned}\int_S -\boldsymbol{T}^A\cdot\boldsymbol{u}^B dS &= -R\int_0^\pi(\sigma_{rr}^A u_r^{BL}+\sigma_{r\theta}^A u_\theta^{BL})d\theta\\ &= i(\lambda+2\mu)k_L R\Omega(k_L R)\{I_1+A_{11}I_2+A_{21}I_3\}\\ &\quad -i\mu k_T R\Omega(k_T R)\{I_4+A_{11}I_5+A_{21}I_6\},\end{aligned} \tag{12a}$$

where we have used the asymptotic expressions for the stress components of the A-field, viz.,

$$\begin{aligned}\sigma_{rr}^A &\approx (\lambda+2\mu)u_{r,r}^A = i(\lambda+2\mu)k_L\Omega(k_L R)A_x^L(\theta),\\ \sigma_{r\theta}^A &\approx \mu u_{\theta,r}^A = i\mu k_T\Omega(k_T R)A_x^T(\theta),\end{aligned} \tag{12b}$$

and a comma preceding a subscript indicates as usual a partial derivative with respect to that subscript. The three terms in each of the curly brackets in Eq. (12a) arise from the three plane waves constituting the B-field, as indicated in Eq. (6a). Consequently, evaluating Eq. (12a) reduces to evaluating the following six integrals:

$$I_1 = \int_0^\pi A_x^L(\theta)\cos(\theta-\theta_0)e^{-ik_L R\cos(\theta-\theta_0)}d\theta, \tag{13a}$$

$$I_2 = \int_0^\pi A_x^L(\theta)\cos(\theta+\theta_0)e^{-ik_L R\cos(\theta+\theta_0)}d\theta, \tag{13b}$$

$$I_3 = \int_0^\pi A_x^L(\theta)\cos(\theta-\psi_0)e^{ik_T R\sin(\theta-\psi_0)}d\theta, \tag{13c}$$

$$I_4 = \int_0^\pi A_x^T(\theta)\sin(\theta-\theta_0)e^{-ik_L R\cos(\theta-\theta_0)}d\theta, \tag{13d}$$

$$I_5 = \int_0^\pi A_x^T(\theta)\sin(\theta+\theta_0)e^{-ik_L R\cos(\theta+\theta_0)}d\theta, \tag{13e}$$

$$I_6 = \int_0^\pi A_x^T(\theta)\sin(\theta-\psi_0)e^{ik_T R\sin(\theta-\psi_0)}d\theta. \tag{13f}$$

For large values of R, these integrals can be evaluated by the stationary phase approximation,[11] which is asymptotically exact, i.e., the neglected terms are negligible compared with the retained term for $kR \gg 1$, where $k = k_L$ or k_T. Thus, for I_1, the stationary phase condition occurs for $\theta = \theta_0$, which leads to

$$I_1 \approx \sqrt{\frac{2\pi i}{k_L R}}A_x^L(\theta_0)e^{-ik_L R}, \tag{14a}$$

whereas for I_2 the stationary phase condition occurs for $\theta = \pi - \theta_0$, leading to

$$I_2 \approx -\sqrt{\frac{2\pi}{ik_L R}}A_x^L(\pi-\theta_0)e^{ik_L R}, \tag{14b}$$

and for I_3 the stationary phase condition occurs for $\theta = \psi_0 + \pi/2$, leading to

$$I_3 \approx 0, \tag{14c}$$

because of the term $\cos(\theta-\psi_0)$ in the integrand.

This last result has an intuitively plausible physical interpretation: it indicates that the cross-work term corresponding to the work done by the radial stress component of state A, which propagates with speed c_L, working through the displacement associated with the mode-converted transverse plane wave of state B, which propagates with a different speed c_T, is asymptotically equal to zero for large R. For the same reason, it is found that

$$I_4 \approx 0, \tag{14d}$$

$$I_5 \approx 0, \tag{14e}$$

whereas

$$I_6 \approx \sqrt{\frac{2\pi}{ik_T R}}A_x^T(\psi_0+\pi/2)e^{ik_T R}. \tag{14f}$$

The same approach can now be used to evaluate the first term on the RHS of Eq. (1), to obtain

$$\begin{aligned}\int_S \boldsymbol{T}^B\cdot\boldsymbol{u}^A dS &= R\int_0^\pi(\sigma_{rr}^{BL}u_r^A+\sigma_{r\theta}^{BL}u_\theta^A)d\theta\\ &= i(\lambda+2\mu)k_L R\Omega(k_L R)\\ &\quad\times\{I_7+A_{11}I_8+A_{21}I_9\}\\ &\quad -i\mu k_T R\Omega(k_T R)\{I_{10}+A_{11}I_{11}+A_{21}I_{12}\}.\end{aligned} \tag{15}$$

It can again be verified that only three of these six new integrals are non-zero, viz., I_7, I_8, and I_{12}. Moreover, two of those non-zero integrals cancel the corresponding terms in Eqs. (14), leading to

$$\begin{aligned}I_1+I_7 &= 2I_1,\\ I_2+I_8 &= 0,\\ I_6+I_{12} &= 0.\end{aligned} \tag{16}$$

These results can now be substituted in Eqs. (12) and (15) to obtain the result previously stated in Sec. II, Eq. (7), thereby completing the required proof.

It can be observed that, although the detailed derivation is lengthy, because it involves a consideration of 12 distinct contributing terms, the final result is very simple: the net contribution to the RHS of Eq. (1) arises from the terms leading to the integrals I_1 and I_7. These terms arise from the counter-propagating longitudinal waves in the two states A and B. The stationary phase approximation results in an effect similar to that of a Dirac delta function, in the sense that the RHS of Eq. (1) only depends on the angular factor $A_x^L(\theta)$ for $\theta = \theta_0$, which is the angle of incidence of the longitudinal plane wave employed for state B, and which also corresponds to the stationary phase condition for I_1 and I_7. The stationary phase approximation also leads to non-zero integrals for the terms corresponding to waves of the same mode propagating in the same direction, but these contributions cancel out between the two terms on the RHS of Eq. (1). These results can be regarded as a generalisation to 2D elasticity of the corresponding result for 1D wave propagation, as presented in Ref. 1, Sec. 1.5, but noting the following differences: (i) there are now two bulk-wave modes, and the non-zero contribution arises only from the counter-propagating waves of the same mode; and (ii) the choice for the auxiliary state now entails specifying a particular angle of incidence, in addition to a direction of propagation, and the contribution from the counter-propagating waves arises only from that particular angle.

The preceding analysis can now be repeated to derive the result stated in Eq. (10) for the transverse wave component of the far field, Eq. (3), by employing as state B the field due to an incident transverse wave, as given by Eq. (9). As noted in Sec. II, the mode-converted wave in this case is an inhomogeneous plane wave for a certain range of incident angles. However, this does not affect the above simple rule, because the mode-converted wave again makes no contribution to the RHS of Eq. (1).

IV. THREE-DIMENSIONAL SOLUTION FOR A BURIED POINT FORCE

There are two points of novelty when applying reciprocity to derive the 3D analogue of the results presented in Sec. II for a 2D buried force, viz., (i) a multi-dimensional generalisation of the stationary phase approximation is required;[33,34] (ii) the auxiliary field must now include the anti-plane field due to the reflection of a shear horizontal (SH) wave,[11–13] in addition to the plane strain fields that were employed in Sec. II. Accordingly, the field that was previously described in Sec. II as being due to a transverse incident wave will now be identified as being due to an incident shear vertical (SV) wave, for clarity.

A. Solution for a horizontal force

Let state A represent the solution of the 3D version of Eqs. (2a) and (2c), with the body force $\boldsymbol{f}$ now specified by

$$f_x = P\delta(x)\delta(y)\delta(z-l),$$
$$f_y = f_z = 0, \tag{17}$$

as shown in Fig. 2, and we again require the solution that satisfies the Sommerfeld radiation condition. Thus, a suitable ansatz for the far field is now

$$u_r^A(r,\theta,\varphi) \approx A_x^L(\theta,\varphi)\Lambda(r;k_L), \tag{18a}$$
$$u_\theta^A(r,\theta,\varphi) \approx A_x^{SV}(\theta,\varphi)\Lambda(r;k_T), \tag{18b}$$
$$u_\varphi^A(r,\theta,\varphi) \approx A_x^{SH}(\theta,\varphi)\Lambda(r;k_T), \tag{18c}$$
$$\Lambda(r;k) = \frac{e^{ikr}}{4\pi r}, \tag{18d}$$

where (r,θ,φ) denote spherical polar coordinates, and $\Lambda(r;k)$ is the free-space Green function for the 3D scalar wave equation, i.e., the 3D analogue of Eq. (4). The corresponding stress components that will be required for evaluating the RHS of Eq. (1) are

$$\sigma_{rr}^A \approx (\lambda+2\mu)u_{r,r}^A = i(\lambda+2\mu)k_L\Lambda(r;k_L)A_x^L(\theta,\varphi), \tag{19a}$$
$$\sigma_{r\theta}^A \approx \mu u_{\theta,r}^A = i\mu k_T\Lambda(r;k_T)A_x^{\mathrm{SV}}(\theta,\varphi), \tag{19b}$$
$$\sigma_{r\varphi}^A \approx \mu u_{\varphi,r}^A = i\mu k_T\Lambda(r;k_T)A_x^{\mathrm{SH}}(\theta,\varphi). \tag{19c}$$

The auxiliary fields chosen for state B are the fields generated by incident plane waves of three different polarisations, identified by superscripts L, SV, and SH. Thus, to determine $A_x^L(\theta,\varphi)$, for a particular direction (θ_0,φ_0), the appropriate B-field is that due to an incident longitudinal wave of unit amplitude given by

$$\boldsymbol{u}^{IL}(x,y,z) = \boldsymbol{d}_0 e^{ik_L\boldsymbol{\alpha}\cdot\boldsymbol{x}},$$
$$\boldsymbol{d}_0 = \boldsymbol{\alpha} = -(\sin\theta_0\cos\varphi_0,\ \sin\theta_0\sin\varphi_0,\ \cos\theta_0). \tag{20}$$

This field is denoted by $\boldsymbol{u}^{BL}(x,y,z;\theta_0,\varphi_0)$, and it is important to note that despite the 3D setting, this is the same 2D plane-strain field that was employed in Sec. II, but rotated about the z-axis through an angle φ_0. Therefore, one can again write

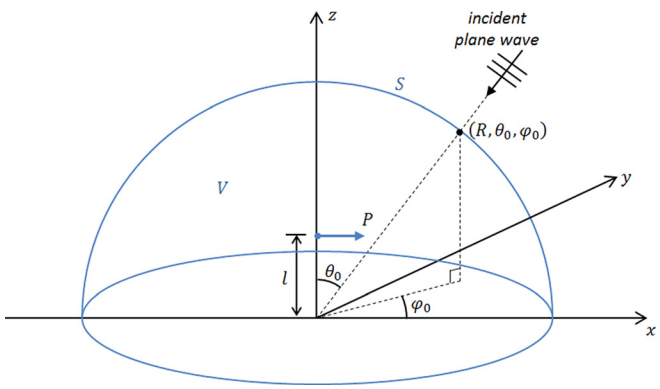

FIG. 2. (Color online) The three-dimensional configuration for a buried point force in a half-space $z \geq 0$ showing the volume V and surface S employed in Eq. (1), as well as the incident plane wave that generates the required auxiliary field.

$$\boldsymbol{u}^{BL}(x,y,z;\theta_0,\varphi_0) = \boldsymbol{u}^{IL} + A_{11}\boldsymbol{u}^{RL} + A_{21}\boldsymbol{u}^{RSV}, \tag{21}$$

where the reflected plane waves $\boldsymbol{u}^{RL}$ and $\boldsymbol{u}^{RSV}$ are also rotated through the same angle φ_0, and the reflection coefficients A_{11}, A_{21} are those given earlier by Eqs. (6e) and (6f), but care is required in transcribing these coefficients, as well as the detailed expressions for the displacement and stress components, due to differences in notation between the 3D case and the 2D case presented in Sec. II. In particular, θ now denotes the polar angle measured from the z-axis, rather than the x axis, and the z-axis now corresponds to the y-axis for the 2D case.

To evaluate Eq. (1), S is taken to be the surface of a hemi-spherical domain V of radius $R > l$, as indicated in Fig. 2. The LHS reduces to $Pu_x^{BL}(0,0,l;\theta_0,\varphi_0)$, by virtue of Eq. (17), and recalling that $\boldsymbol{f}^B = \boldsymbol{0}$. As for the RHS, the integral over the flat portion $z = 0$ again vanishes by virtue of the boundary condition in Eq. (2c), which applies for both states A and B, leaving the integral over the hemi-spherical surface, which can be expressed as follows:

$$\text{RHS Eq.}(1) = R^2 \int_0^{2\pi}\int_0^{\pi/2} (\boldsymbol{T}^B\cdot\boldsymbol{u}^A - \boldsymbol{T}^A\cdot\boldsymbol{u}^B)\sin\theta d\theta d\varphi. \tag{22a}$$

Each of the terms in this integral involves several contributions arising from the various plane waves comprising the B-field, which leads to integrals involving different exponentials. For example, the second term of Eq. (22a) leads to

$$-R^2 \int_0^{2\pi}\int_0^{\pi/2} (\sigma_{rr}^A u_r^{BL} + \sigma_{r\theta}^A u_\theta^{BL} + \sigma_{r\varphi}^A u_\varphi^{BL})\sin\theta d\theta d\varphi. \tag{22b}$$

Using Eqs. (19)–(21), the first term of this expression can be further expanded as follows:

$$\begin{aligned} &-R^2 \int_0^{2\pi}\int_0^{\pi/2} \sigma_{rr}^A u_r^{BL}\sin\theta d\theta d\varphi \\ &\quad = i(\lambda+2\mu)k_L R^2 \Lambda(R;k_L)\{I_1 + A_{11}I_2 + A_{21}I_3\}. \end{aligned} \tag{22c}$$

Here I_1 is the 3D analogue of the integral defined by Eq. (13a), which is now given by

$$I_1 = \int_0^{2\pi}\int_0^{\pi/2} A_x^L(\theta,\varphi)e^{-ik_L R\cos\chi}\cos\chi\sin\theta d\theta d\varphi, \tag{23a}$$

$$\cos\chi = \hat{\boldsymbol{r}}_0\cdot\hat{\boldsymbol{x}} = \sin\theta\sin\theta_0\cos(\varphi-\varphi_0) + \cos\theta\cos\theta_0, \tag{23b}$$

where χ denotes the angle between the unit vectors $\hat{\boldsymbol{r}}_0 = -\boldsymbol{\alpha}$, and $\hat{\boldsymbol{x}} = \boldsymbol{x}/|\boldsymbol{x}|$, and $\hat{\boldsymbol{r}}_0$ can be regarded as pointing in the direction of the source of the incident plane wave. The integrals I_2 and I_3 are similarly the 3D analogues of the integrals defined by Eqs. (13b) and (13c), with the exponential terms in these integrals again arising from expressing a plane wave in terms of spherical polar coordinates. These integrals can be evaluated asymptotically for large kR by an extension of the stationary phase approximation to multi-dimensional integrals.[33,34] For the purposes of illustration, it will suffice to note here the result for I_1, which arises from the stationary phase condition for $\theta = \theta_0, \varphi = \varphi_0$, so that $\cos\chi = 1$,

$$I_1 \approx i2\pi A_x^L(\theta_0,\varphi_0)\frac{e^{-ik_L R}}{k_L R}. \tag{23c}$$

Each of the three terms in Eq. (22b) will lead to three integrals, and the first term in Eq. (22a) will also lead to nine integrals. For brevity, these integrals will not be presented in detail here. It is sufficient to note that the stationary phase approximation again leads to the same conclusion as in Sec. III for the 2D case, viz., (i) integrals like I_3 arising from cross terms involving waves of different modes vanish asymptotically; (ii) integrals like I_2 arising from cross terms involving waves of the same mode propagating in the same direction are non-zero, but these contributions cancel out between the two terms in Eq. (22a). Thus, the simple rule again applies: the RHS of Eq. (1) can be evaluated by using double the value associated with the integral I_1 which arises from counter-propagating waves of the same mode. This leads to the result

$$Pu_x^{BL}(0,0,l;\theta_0,\varphi_0) = -(\lambda+2\mu)A_x^L(\theta_0,\varphi_0), \tag{24}$$

thereby providing an explicit solution for $A_x^L(\theta,\varphi)$ in terms of the known B-field.

This procedure can now be repeated to determine the two other angular functions in Eqs. (18b) and (18c). However, the pattern for this derivation is now clear, and it will suffice to record next the result for the general case of a buried force.

B. Solution for a point force of arbitrary orientation

For ease of reference, we shall summarize here the problem formulation as well as the solution obtained by applying the reciprocal relation in Eq. (1).

The far-field displacements corresponding to the solution of the 3D time-harmonic equations of motion for an arbitrarily oriented point force given by

$$(\lambda+\mu)\nabla\nabla\cdot\boldsymbol{u} + \mu\nabla^2\boldsymbol{u} + \rho\omega^2\boldsymbol{u} = -\boldsymbol{f}, \tag{25a}$$

$$\boldsymbol{f} = \boldsymbol{F}\delta(\boldsymbol{x}-\boldsymbol{\xi}), \quad \boldsymbol{\xi} = (\xi,\eta,\zeta), \quad \zeta > 0, \tag{25b}$$

in a half-space $z > 0$ subject to the traction-free boundary condition.

$$\boldsymbol{T} = \sigma_{ji}n_j = \boldsymbol{0} \quad \text{on} \quad z = 0, \tag{25c}$$

with $\boldsymbol{n} = (0,0,-1)$, and the Sommerfeld radiation condition, can be derived from Eq. (1) in the following form:

$$u_r(r,\theta,\varphi) \approx A^L(\theta,\varphi)\Lambda(r;k_L), \tag{26a}$$

$$u_\theta(r,\theta,\varphi) \approx A^{SV}(\theta,\varphi)\Lambda(r;k_T), \tag{26b}$$

$$u_\varphi(r,\theta,\varphi) \approx A^{SH}(\theta,\varphi)\Lambda(r;k_T), \tag{26c}$$

$$\Lambda(r;k) = \frac{e^{ikr}}{4\pi r}, \tag{26d}$$

with

$$A^L(\theta_0,\varphi_0) = -\frac{1}{\lambda+\mu}\boldsymbol{F}\cdot\boldsymbol{u}^{BL}(\boldsymbol{\xi};\hat{\boldsymbol{r}}_0), \tag{26e}$$

$$A^{\mathrm{SV}}(\theta_0,\varphi_0) = -\frac{1}{\mu}\boldsymbol{F}\cdot\boldsymbol{u}^{\mathrm{BSV}}(\boldsymbol{\xi};\hat{\boldsymbol{r}}_0), \tag{26f}$$

$$A^{\mathrm{SH}}(\theta_0,\varphi_0) = -\frac{1}{\mu}\boldsymbol{F}\cdot\boldsymbol{u}^{\mathrm{BSH}}(\boldsymbol{\xi};\hat{\boldsymbol{r}}_0), \tag{26g}$$

$$\hat{\boldsymbol{r}}_0 = (\sin\theta_0\cos\varphi_0,\ \sin\theta_0\sin\varphi_0,\ \cos\theta_0), \tag{26h}$$

where $\boldsymbol{u}^{BL}$,$\boldsymbol{u}^{\mathrm{BSV}}$, $\boldsymbol{u}^{\mathrm{BSH}}$, denote, respectively, the auxiliary fields generated by an incident longitudinal, shear vertical, and shear horizontal plane wave, with propagation direction given by $-\hat{\boldsymbol{r}}_0$. The fields $\boldsymbol{u}^{BL}$,$\boldsymbol{u}^{\mathrm{BSV}}$ are the plane-strain fields given by Eqs. (6) and (9) but rotated around the z-axis through an angle φ_0, keeping in mind the differences in notation between the 3D and 2D coordinates. The field $\boldsymbol{u}^{BSH}$ is similarly obtained by rotating the anti-plane field due to an incident unit amplitude shear-horizontal plane wave in a traction-free half-space.[11–13] Thus, by reducing the solution for a buried point force to the well-known solutions for plane wave reflection in a traction-free half space, the reciprocal relation Eq. (1) can justifiably be claimed to provide a simpler solution than would be obtained from a direct application of integral transform techniques.

V. SOLUTION FOR BURIED CRACKS

The solution derived in Sec. IV for a point force provides the Green function that underpins representation theorems for the radiated or scattered field due to crack-like sources and scatterers,[20,21,23–25] as well as volume sources and inhomogeneities,[21,22] in a half-space. In particular, a crack or delamination can be modelled as an open surface Σ across which the elastic displacement can be discontinuous. This discontinuity is quantified by

$$\Delta\boldsymbol{u}(\boldsymbol{x}) = \boldsymbol{u}^{+}(\boldsymbol{x}) - \boldsymbol{u}^{-}(\boldsymbol{x}), \tag{27a}$$

where $\boldsymbol{u}^{+}$ denotes the displacement on the top face of Σ, as indicated by the specified direction for the normal vector $\boldsymbol{n}$ in Fig. 3, and $\boldsymbol{u}^{-}$ denotes the displacement on the bottom face. The time-harmonic scattered field due to the crack can then be expressed as follows:[20,21]

$$u_m(\boldsymbol{x}) = \int_\Sigma \Delta u_i(\boldsymbol{\xi}) c_{ijkl} G_{mk,l}(\boldsymbol{x};\boldsymbol{\xi}) n_j d\Sigma(\boldsymbol{\xi}), \tag{27b}$$

where c_{ijkl} denotes the elasticity tensor, which can be expressed in terms of the Lamé parameters for an isotropic material,

$$c_{ijkl} = \lambda\delta_{ij}\delta_{kl} + \mu(\delta_{ik}\delta_{jl} + \delta_{il}\delta_{jk}), \tag{27c}$$

whereas $G_{ij}(\boldsymbol{x};\boldsymbol{\xi})$ denotes the Green function representing the ith component of displacement at a field point $\boldsymbol{x}$ due to the jth component of force applied at the point $\boldsymbol{\xi}$, and $d\Sigma(\boldsymbol{\xi})$ denotes an infinitesimal element of area on the surface Σ. The displacement discontinuity that serves as the source strength in Eq. (27b) must generally be determined computationally. In the case of the radiated field due to crack growth, the time evolution of the surface Σ must also be determined, which requires a time-domain formulation.[26–29] However, valuable insights can often be obtained by using various approximations. In particular, it is useful to consider the point-scatterer limit for which the source strength can be specified in terms of Dirac delta functions.

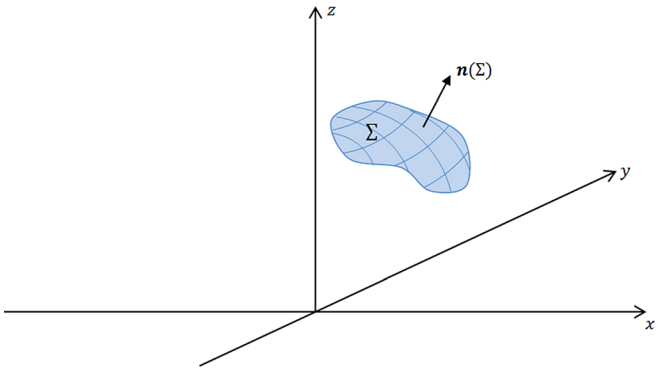

FIG. 3. (Color online) A surface of displacement discontinuity Σ, representing a crack or delamination in a half-space $z \geq 0$.

A case of particular interest is a Mode I (tensile) crack element, with the crack surface Σ lying in the yz-plane, i.e., $\boldsymbol{n} = (1,0,0)$ in Fig. 3, which can be specified as follows

$$\begin{aligned} &\Delta u_x = U\delta(y)\delta(z-l) \quad \text{on} \quad x = 0, \\ &\Delta u_y = \Delta u_z = 0, \end{aligned} \tag{28}$$

where the source strength U represents the crack volume, i.e., the integral of the crack opening Δu_x over the area Σ, which can be estimated by a quasi-static approximation for small cracks (relative to the wavelength),[31] and the location $(0,0,l)$ can be regarded as the centroid for this volume. On substituting Eq. (28) into Eq. (27), the integral can be interpreted as the field due to a particular combination of force doublets (or dipoles) as shown in Fig. 4.[20,21] This equivalence means that the field due to the crack element in Eq. (28) can also be specified as the solution of Eq. (25a) with the body force specified as follows:

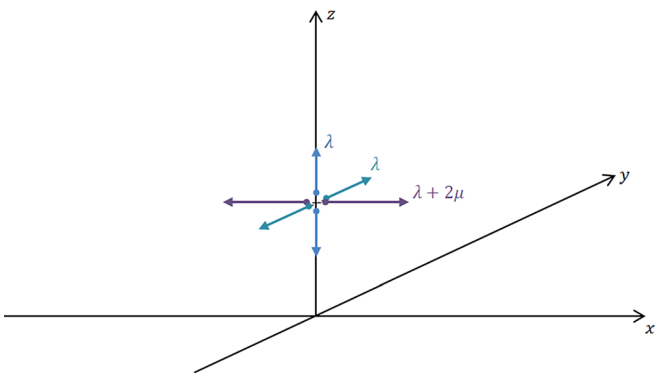

FIG. 4. (Color online) The force doublets comprising the body force equivalent for a Mode I crack element, with the crack lying in the plane $x = 0$.

$$f_x = -(\lambda + 2\mu)U\delta'(x)\delta(y)\delta(z-l), \tag{29a}$$

$$f_y = -\lambda U\delta(x)\delta'(y)\delta(z-l), \tag{29b}$$

$$f_z = -\lambda U\delta(x)\delta(y)\delta'(z-l). \tag{29c}$$

The advantage of this alternative specification is that the field can be easily derived by applying Eq. (1). Consider, for example, the case of a horizontal doublet, specified by

$$\begin{aligned} f_x &= -(\lambda + 2\mu)U\delta'(x)\delta(y)\delta(z-l), \\ f_y &= f_z = 0. \end{aligned} \tag{30}$$

By following the approach presented in Sec. IV A for a horizontal force, one would now obtain, instead of Eq. (24),

$$U(\lambda + 2\mu)u^{BL}_{x,x}(0,0,l;\theta_0,\varphi_0) = (\lambda + 2\mu)A^L_x(\theta_0,\varphi_0). \tag{31}$$

The reason for retaining the factor $(\lambda + 2\mu)$ on both sides of Eq. (31) is to make it easier to see that by summing the contributions from the three doublets in Eq. (29), one would obtain

$$U\sigma^{BL}_{xx}(0,0,l;\theta_0,\varphi_0) = (\lambda + 2\mu)A^L_x(\theta_0,\varphi_0). \tag{32}$$

This derivation can be repeated for the other angular functions to show that the far field due to the Mode I crack element specified by Eq. (28), or equivalently by Eq. (29), is given by the ansatz in Eq. (18) with

$$A^L_x(\theta_0,\varphi_0) = \frac{1}{\lambda + 2\mu}U\sigma^{BL}_{xx}(0,0,l;\theta_0,\varphi_0), \tag{33a}$$

$$A^{SV}_x(\theta_0,\varphi_0) = \frac{1}{\mu}U\sigma^{BSV}_{xx}(0,0,l;\theta_0,\varphi_0), \tag{33b}$$

$$A^{SH}_x(\theta_0,\varphi_0) = \frac{1}{\mu}U\sigma^{BSH}_{xx}(0,0,l;\theta_0,\varphi_0). \tag{33c}$$

The fact that only the σ_{xx} component of the respective auxiliary fields is required for this solution is intuitively plausible: it is only that stress component that does work against the Mode I crack opening Δu_x for a crack lying in the yz-plane. Although this result has been derived here in the context of the bulk-wave contributions to the far field, it can readily be verified that it also applies for the surface wave contribution, i.e., the reciprocity approach for deriving the surface motions due to a buried Mode I crack element specified by Eq. (28) will only require the σ_{xx} component of the Rayleigh wave field, which serves as the auxiliary field. This result appears to have been overlooked in previous work.[10]

The preceding observation for the field due to a Mode I crack element paves the way for the following generalisation which can be derived by applying Eq. (1) in conjunction with the body-force equivalent for displacement discontinuities. The far field due to a crack element specified by the displacement discontinuity

$$\Delta\boldsymbol{u} = \boldsymbol{U}\delta(\boldsymbol{x} - \boldsymbol{\xi}), \quad \boldsymbol{\xi} = (\xi,\eta,\zeta), \quad \zeta > 0, \tag{34a}$$

across a surface with normal $\boldsymbol{n}$, is given by Eqs. (26a)–(26d) with

$$A^L(\theta_0,\varphi_0) = \frac{1}{\lambda + 2\mu}U_j\sigma^{BL}_{ji}(\boldsymbol{\xi};\hat{\boldsymbol{r}}_0)n_i, \tag{34b}$$

$$A^{SV}(\theta_0,\varphi_0) = \frac{1}{\mu}U_j\sigma^{BSV}_{ji}(\boldsymbol{\xi};\hat{\boldsymbol{r}}_0)n_i, \tag{34c}$$

$$A^{SH}(\theta_0,\varphi_0) = \frac{1}{\mu}U_j\sigma^{BSH}_{ji}(\boldsymbol{\xi};\hat{\boldsymbol{r}}_0)n_i. \tag{34d}$$

Whilst this result is of interest in its own right, as a point-scatterer approximation for buried cracks, it can also be used as the building block for representing the far field due to an arbitrary displacement discontinuity $\Delta\boldsymbol{u}(\boldsymbol{x})$ across an arbitrary surface Σ, as shown in Fig. 3. This far field is again given by Eqs. (26a)–(26d) with

$$A^L(\theta_0,\varphi_0) = \frac{1}{\lambda + 2\mu}\int_\Sigma U_j(\boldsymbol{\xi})\sigma^{BL}_{ji}(\boldsymbol{\xi};\hat{\boldsymbol{r}}_0)n_i d\Sigma(\boldsymbol{\xi}), \tag{35a}$$

$$A^{SV}(\theta_0,\varphi_0) = \frac{1}{\mu}\int_\Sigma U_j(\boldsymbol{\xi})\sigma^{BSV}_{ji}(\boldsymbol{\xi};\hat{\boldsymbol{r}}_0)n_i d\Sigma(\boldsymbol{\xi}), \tag{35b}$$

$$A^{SH}(\theta_0,\varphi_0) = \frac{1}{\mu}\int_\Sigma U_j(\boldsymbol{\xi})\sigma^{BSH}_{ji}(\boldsymbol{\xi};\hat{\boldsymbol{r}}_0)n_i d\Sigma(\boldsymbol{\xi}). \tag{35c}$$

Thus, by using the reciprocal relation in Eq. (1), it has been possible to derive a very general formula for the scattered far field due to a buried crack in a half-space, in terms of (i) the stress fields associated with plane wave reflection in a half-space, which are well known, and (ii) the displacement discontinuity across the crack, which needs to be determined computationally, or estimated by various approximations.

VI. DISCUSSION AND CONCLUSION

It has been shown that the elastodynamic reciprocal relation expressed by Eq. (1) leads to a compact solution for the far field due to a buried point force in a half-plane or half-space. This solution involves the displacements associated with auxiliary fields corresponding to plane wave reflection in the half-space, for incident waves of longitudinal, shear-vertical, or shear-horizontal polarisation. These are well known two-dimensional fields (plane strain for incident longitudinal and shear-vertical waves; anti-plane strain for an incident shear-horizontal wave), which must be rotated through the azimuthal angle φ_0 to obtain the 3D solution for a buried force. This solution for a point force in turn provides the Green function for representing the far field due to more general buried sources or scatterers. In particular, it was shown that the far field for crack-like scatterers can be expressed in terms of the displacement discontinuity across the crack and the associated stress components of the auxiliary fields. Thus, the use of reciprocity can justifiably be claimed to provide a simpler and more elegant solution than alternative approaches based for example on integral transform techniques.

Clearly, the reciprocity approach can also be used to advantage to derive the far field for other configurations involving a semi-infinite or infinite domain, provided that the required auxiliary fields corresponding to plane wave incidence are again available in a convenient analytical form. This includes the case of a half-space covered by a thin layer, as well as two half-spaces joined by a thin layer, or by an interface with a linear traction law.[41] Furthermore, this also includes the case of buried sources or scatterers located at, or close to, the boundary of a circular or spherical hole, for which analytical solutions are available for the problem of plane wave incidence.[32] Thus, the present work has a wide-ranging scope for practical applications in nondestructive evaluation and structural health monitoring.

Finally, although the focus in the present work has been on deriving the bulk-wave contributions to the far field, it is worth noting that the present approach would also provide a more direct derivation, relative to that presented in Refs. 1–5, for the surface wave motion due to a buried force in a half-space, and the Lamb-wave modes generated by an arbitrarily directed force in an elastic layer, in the sense that it is not necessary to resort to constructing a field corresponding to the sum of an outgoing and an incoming circular-crested wave. Instead, the auxiliary field can be taken to be a plane wave, the crucial step being the use of the stationary phase approximation to evaluate the RHS of Eq. (1).

[1]J. D. Achenbach, *Reciprocity in Elastodynamics* (Cambridge University Press, Cambridge, UK, 2003), pp. 1–255.
[2]J. D. Achenbach and Y. Xu, "Use of elastodynamic reciprocity to analyse point-load generated axisymmetric waves in a plate," Wave Motion **30**, 57–67 (1999).
[3]J. D. Achenbach and Y. Xu, "Wave motion in an isotropic elastic layer generated by a time-harmonic point load of arbitrary direction," J. Acoust. Soc. Am. **106**, 83–90 (1999).
[4]J. D. Achenbach, "Calculation of surface wave motions due to a subsurface point force: An application of elastodynamic reciprocity," J. Acoust. Soc. Am. **107**, 1892–1897 (2000).
[5]J. D. Achenbach, "Laser excitation of surface wave motion," J. Mech. Phys. Solids **51**, 1885–1902 (2003).
[6]I. Arias and J. D. Achenbach, "Thermoelastic generation of ultrasound by line-focused laser irradiation," Int. J. Solids Structures **40**, 6917–6935 (2003).
[7]I. Arias and J. D. Achenbach, "Rayleigh wave correction for the BEM analysis of two-dimensional elastodynamic problems in a half-space," Int. J. Numer. Meth. Eng. **60**, 2131–2140 (2004).
[8]H. Phan, Y. Cho, and J. D. Achenbach, "Validity of the reciprocity approach for determination of surface wave motion," Ultrasonics **53**, 665–671 (2013).
[9]H. Phan, Y. Cho, and J. D. Achenbach, "Verification of surface wave solutions obtained by the reciprocity theorem," Ultrasonics **54**, 1891–1894 (2014).
[10]H. Zhang and J. D. Achenbach, "Use of equivalent body forces for acoustic emission from a crack in a plate," Mech. Research Commun. **68**, 105–108 (2015).
[11]J. D. Achenbach, *Wave Propagation in Elastic Solids* (North-Holland, Amsterdam, 1973), Chap. 5.
[12]K. F. Graff, *Wave Motion in Elastic Solids* (Ohio State University Press, Columbus, OH, 1975), Chap. 5.
[13]J. L. Rose, *Ultrasonic Waves in Solid Media* (Cambridge University Press, New York, 1999), Chap. 4.
[14]Z. Su and L. Ye, *Identification of Damage Using Lamb Waves* (Springer, Berlin, 2009), pp. 1–346.
[15]V. Giurgiutiu, *Structural Health Monitoring with Piezoelectric Wafer Active Sensors* (Elsevier Academic, Boston, 2014), pp. 1–747.
[16]N. Nadarajah, B. S. Vien, W. K. Chiu, and L. R. F. Rose, "Scattering phenomena of edge guided waves at and around notches," Adv. Mater. Res. **891-892**, 1249–1254 (2014).
[17]W. K. Chiu, L. R. F. Rose, and N. Nadarajah, "Scattering of the fundamental anti-symmetric Lamb wave by a mid-plane edge delamination in a fiber-composite laminate," Proc. Eng. **188**, 317–324 (2017).
[18]B. S. Vien, N. Nadarajah, W. K. Chiu, and L. R. F. Rose, "Scattering of the fundamental symmetric wave mode incident on a defect on the blind side of a weep hole in an isotropic plate," Adv. Mater. Res. **891-892**, 1237–1242 (2014).
[19]W. K. Chiu, L. R. F. Rose, and B. S. Vien, "Scattering of the edge-guided wave by an edge crack at a circular hole in an isotropic plate," Proc. Eng. **188**, 309–316 (2017).
[20]R. Burridge and L. Knopoff, "Body force equivalents for seismic dislocations," Bull. Seismological Soc. Am. **54**, 1875–1888 (1964).
[21]K. Aki and P. G. Richards, *Quantitative Seismology* (Freeman, San Francisco, CA, 1980), Chap. 3.
[22]R. Wu and K. Aki, "Scattering characteristics of elastic waves by an elastic heterogeneity," Geophysics **50**, 582–595 (1985).
[23]D. Guo, A. K. Mal, and K. Ono, "Wave theory of acoustic emission in composite laminates," J. Acoust. Emiss. **14**, S19–S46 (1996).
[24]J. D. Achenbach, A. K. Gautesen, and H. McMaken, *Ray Methods for Waves in Elastic Solids* (Pitman, Boston, MA, 1982), pp. 1–251.
[25]L. W. Schmerr, *Fundamentals of Ultrasonic Nondestructive Evaluation* (Plenum, New York, 1998), Chap. 10.
[26]L. R. F. Rose, "On the acoustic emission due to the fracture of brittle inclusions," J. Nondestr. Eval. **1**, 149–155 (1980).
[27]L. R. F. Rose, "The stress-wave radiation from growing cracks," Int. J. Fract. **17**, 45–60 (1981).
[28]S. Hirose and J. D. Achenbach, "Time-domain boundary element analysis of elastic wave interaction with a crack," Int. J. Numer. Methods Eng. **28**, 629–644 (1989).
[29]S. Hirose and J. D. Achenbach, "Higher harmonics in the far field due to dynamic crack-face contacting," J. Acoust. Soc. Am. **93**, 142–147 (1993).
[30]C. Schaal, H. Samajder, H. Baid, and A. K. Mal, "Rayleigh to Lamb wave conversion at a delamination-like crack," J. Sound Vib. **353**, 150–163 (2015).
[31]M. T. Resch, J. C. Shyne, G. S. Kino, and D. V. Nelson, "Long wavelength Rayleigh wave scattering from microscopic surface fatigue cracks," Rev. Progr. Quant. Nondestr. Eval. **1**, 573–578 (1982).
[32]Y. H. Pao and C. C. Mow, *Diffraction of Elastic Waves and Dynamic Stress* Concentrations (Crane Russak, New York, 1973), Chap. 5.
[33]D. S. Jones and M. Kline, "Asymptotic expansion of multiple integrals and the method of stationary phase," J. Math. Phys. **37**, 1–28 (1958).
[34]N. Bleistein and R. A. Handelsman, *Asymptotic Expansions of Integrals* (Holt, Rinehart and Winston, New York, 1975), Chap. 8.
[35]T. D. Mast, A. I. Nachman, and R. C. Waag, "Focusing and imaging using a time-domain eigenfunction method," J. Acoust. Soc. Am. **102**, 715–725 (1997).
[36]F. Lin, A. I. Nachman, and R. C. Waag, "Quantitative imaging using a time-domain eigenfunctions method," J. Acoust. Soc. Am. **108**, 899–912 (2000).
[37]L. R. F. Rose and C. H. Wang, "Mindlin plate theory for damage detection: Imaging of flexural inhomogeneities," J. Acoust. Soc. Am. **127**, 754–763 (2010).
[38]L. R. F. Rose, E. Chan, and C. H. Wang, "A comparison and extensions of algorithms for quantitative imaging of laminar damage in plates. I. Point spread functions and near field imaging," Wave Motion **58**, 222–243 (2015).
[39]E. R. Lapwood, "The disturbance due to a line source in a semi-infinite elastic medium," Philos. Trans. R. Soc. London Ser. A **242**, 1–42 (1949).
[40]L. R. F. Rose, "Point source representation for laser-generated ultrasound," J. Acoust. Soc. Am. **75**, 723–732 (1984).
[41]J. M. Baik and R. B. Thompson, "Ultrasonic scattering from imperfect interfaces: A quasi-static model," J. Nondestr. Eval. **4**, 177–196 (1984).